

The Global Nonhydrostatic Model **NICAM**

Numerics and performance of its dynamical core

Frontier Research Center for Global Change
Hirofumi TOMITA



- Motivation of our new modeling
 - Global cloud resolving model
- Dynamical core
 - Horizontal grid configuration
 - Validation by shallow water model
 - Nonhydrostatic framework
 - Test case result
 - Held-Suarez Test Case
 - Life cycle of baroclinic wave
 - Computational performance
- Strategy of development of physical process
 - Use of horizontal stretched grid
 - Tropical squall-line experiment
 - Fast path to achieve our model development
- Summary and Future plan



■ General problem for current AGCMs

■ Cumulus parameterization

- One of ambiguous factors
- Statistical closure of cumulus

■ Future AGCM

■ Explicit treatment of each cloud

- Cumulus parameterization
Large scale condensation scheme : not used!
- Cloud microphysics : used!

■ Explicit treatment of multi-scale interactions

- Each cloud scale → meso-scale → planetary scale

→ *Global Cloud Resolving Model*



■ Target resolutions

- 5 km or less in the horizontal direction
- Several 100 m in the vertical

■ Strategy of dycore development

■ Quasi-uniform grid

- Spectral method :
not efficient in high resolution simulations.
 - Legendre transformation
 - Massive data transfer between computer nodes
- Latitude-longitude grid :
the pole problem.
 - Severe limitation of time interval by the CFL condition.
- The icosahedral grid:
homogeneous grid over the sphere
 - To avoid the pole problem.

■ Non-hydrostatic equations system

- Very high resolution in horizontal direction.



■ Global Shallow Water Model

- To examine the potential of icosahedral grid.
(Tomita et al. (2001,2002) *J.Compt.Phys.*)
 - Test bed for development of numerical scheme (e.g. advection scheme) on the icosahedral grid.

■ Regional Non-hydrostatic Model

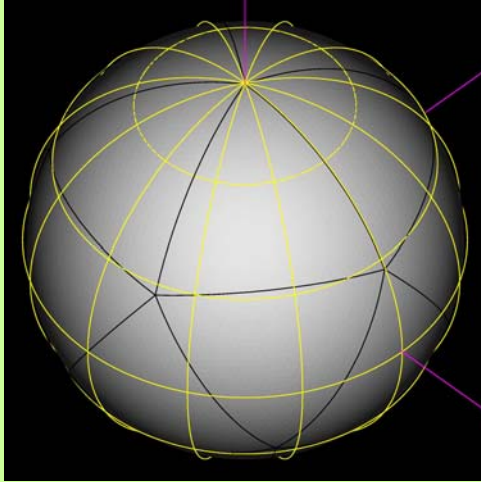
- To examine a numerical non-hydrostatic scheme suitable to climate model.
(Satoh(2002,2003) *Mon.Wea.Rev.*)
 - Test bed for development and validation of new physical parameterizations.

■ Global Non-hydrostatic Model

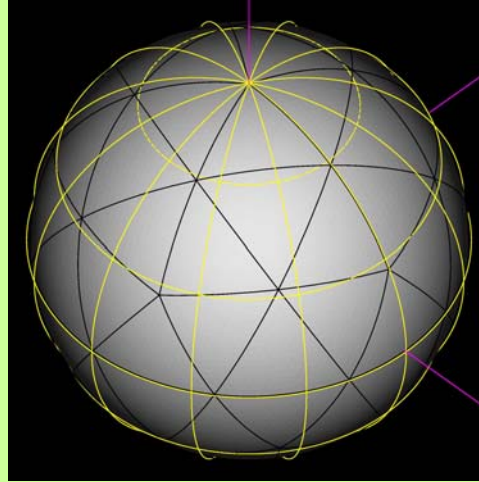
- Base on **our non-hydrostatic scheme**
- Using **the icosahedral grid configuration** in the horizontal direction.
(Tomita & Satoh (2004) *Fluid Dyn.Res.*)



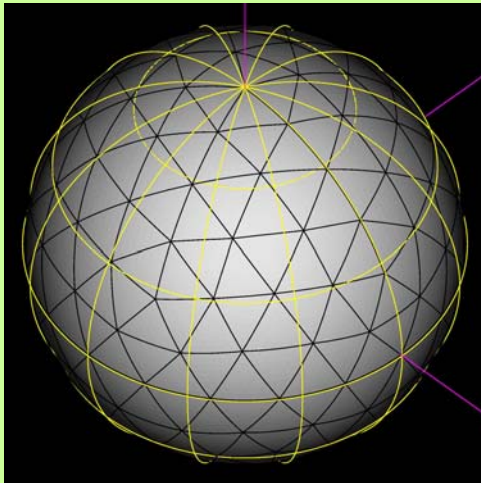
(0) grid division level 0



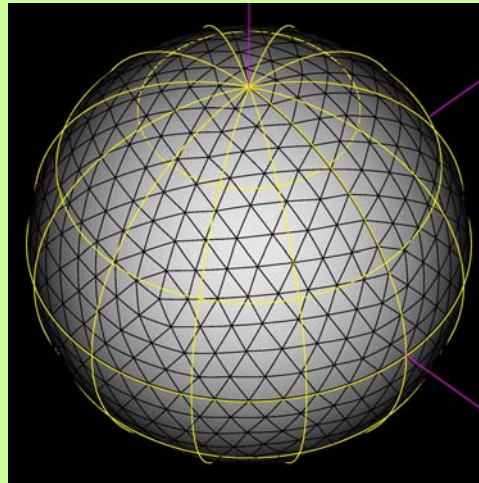
(1) grid division level 1



(2) grid division level 2



(3) grid division level 3



■ Grid generation

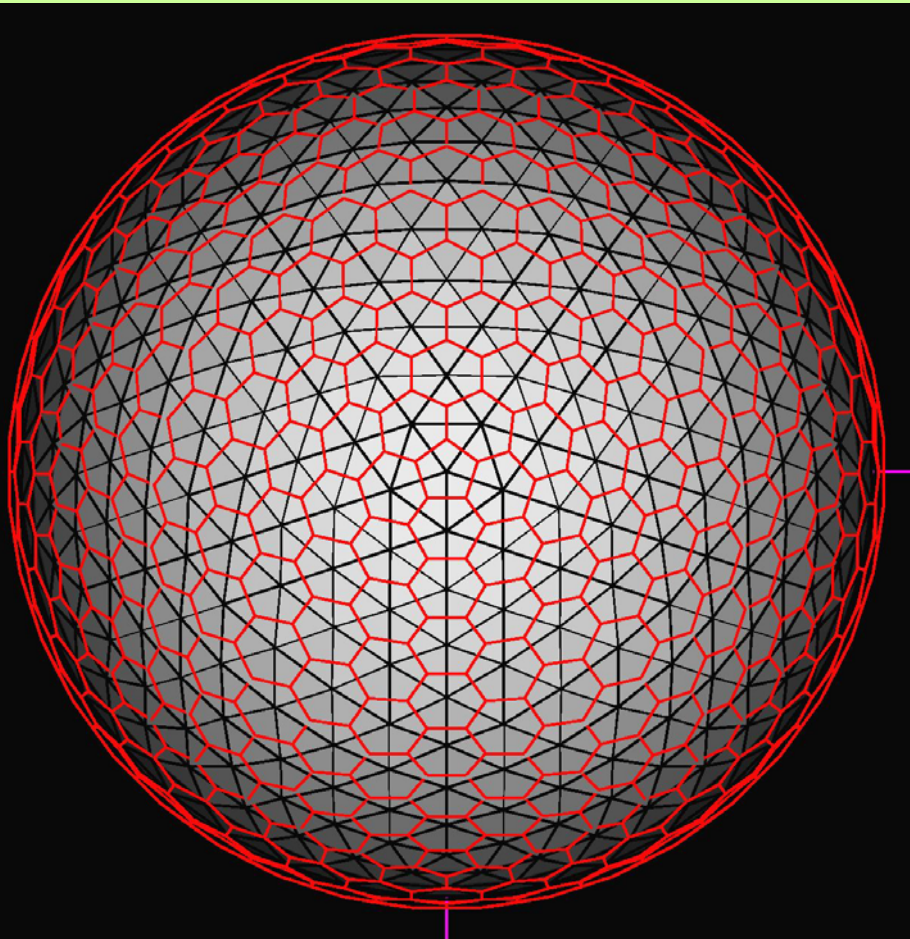
1. Start from the spherical icosahedron.
(glevel-0)
2. Connection of the mid-points of the geodesic arc
→ 4 sub-triangle
(glevel-1)
3. Iteration of this process
→ A finer grid structure
(glevel-n)

STD-grid

■ # of gridpoints

- 11 iterations are required
to obtain the 5km grid
interval.





Glevel-3 grid & control volume

Arakawa A-grid type

■ Velocity, mass

- triangular vertices

■ Control volume

- Connection of center of triangles
 - Hexagon
 - Pentagon at the icosahedral vertices

Advantage

■ Easy to implement

■ Less computational mode

- Same number of grid points for vel. and mass

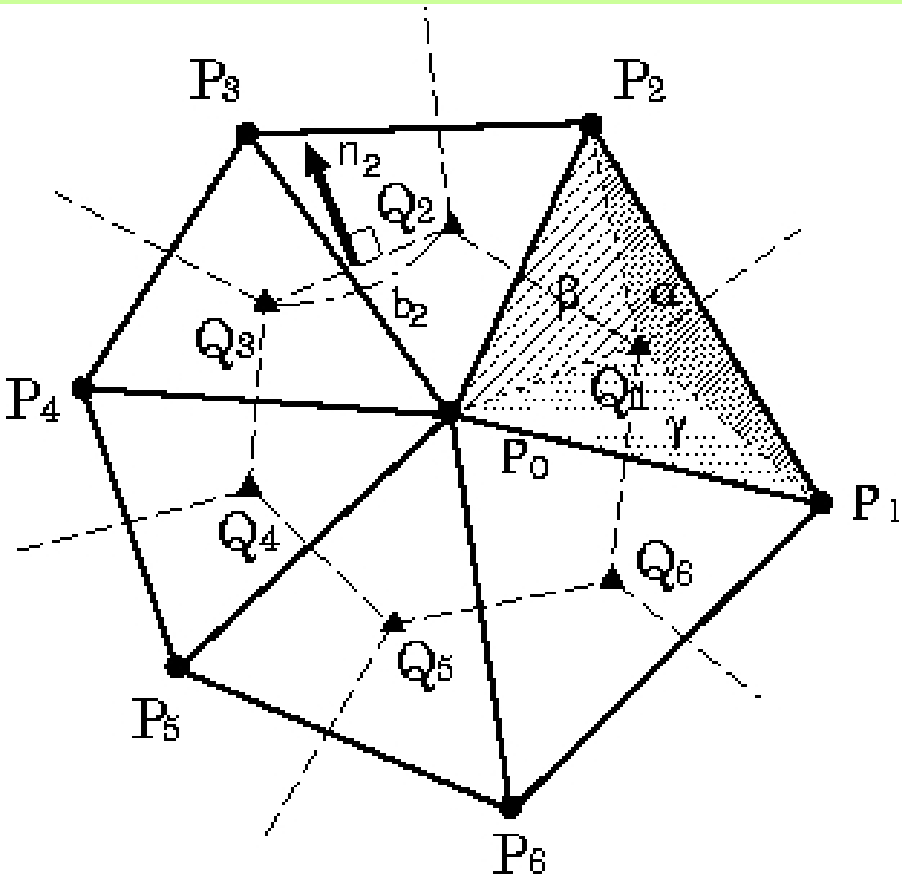
Disadvantage

■ Non-physical

2-grid scale structure

- E.g. bad geostrophic adjustment





■ e.g. Divergence

1. Vector : given at P_i

$$\mathbf{u}(P_i)$$

2. Interpolation of u at Q_i

$$\mathbf{u}(Q_i) \approx \frac{\alpha \mathbf{u}(P_0) + \beta \mathbf{u}(P_i) + \gamma \mathbf{u}(P_{1+\text{mod}(i,6)})}{\alpha + \beta + \gamma}$$

3. Gauss theorem

$$\nabla \cdot \mathbf{u}(P_0) \approx \frac{1}{A(P_0)} \sum_{i=1}^6 b_i \frac{\mathbf{u}(Q_i) + \mathbf{u}(Q_{1+\text{mod}(i,6)})}{2} \cdot \mathbf{n}_i$$

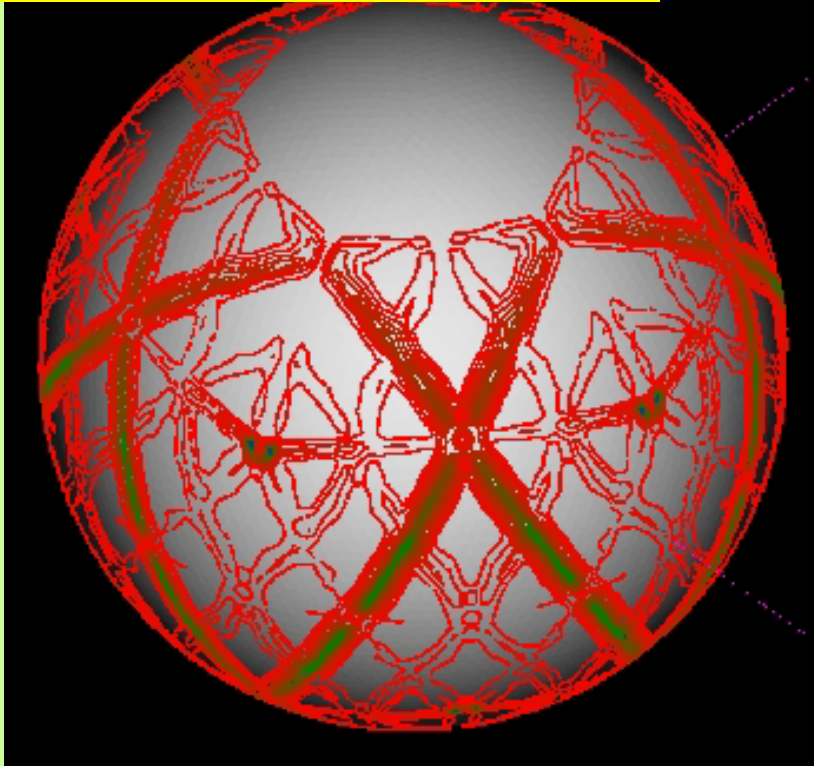
2nd order accuracy?

NO

→ Allocation points is not gravitational center (default grid)

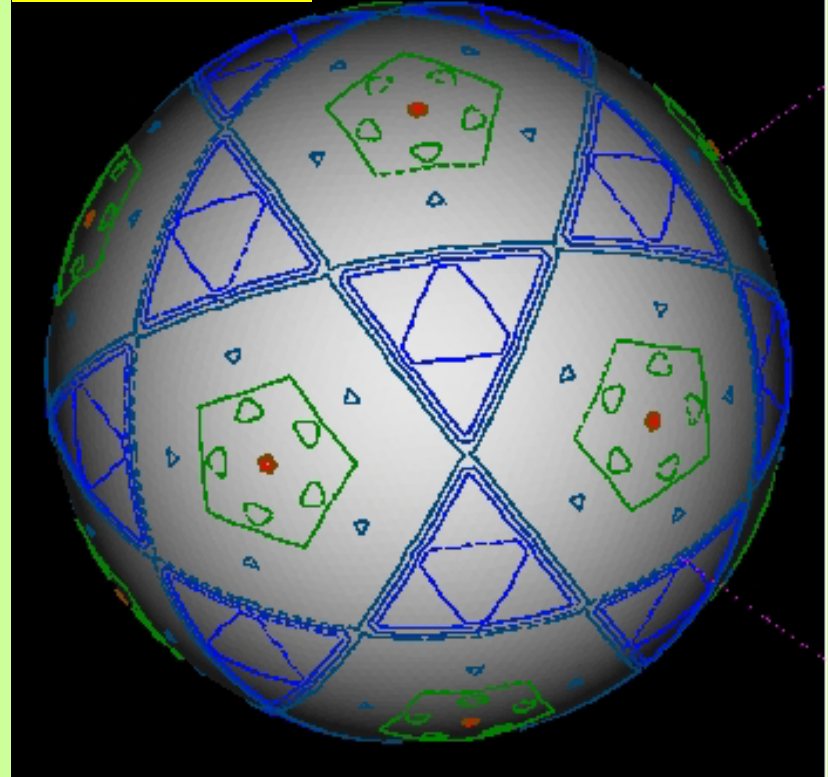


Error of divergence operator



- Error of div operator
 - Large error on the original icosahedral arc
 - Fractal distribution
 - Generation of grid noise

Area of CV



- Distribution of CV area
 - Fractal distribution

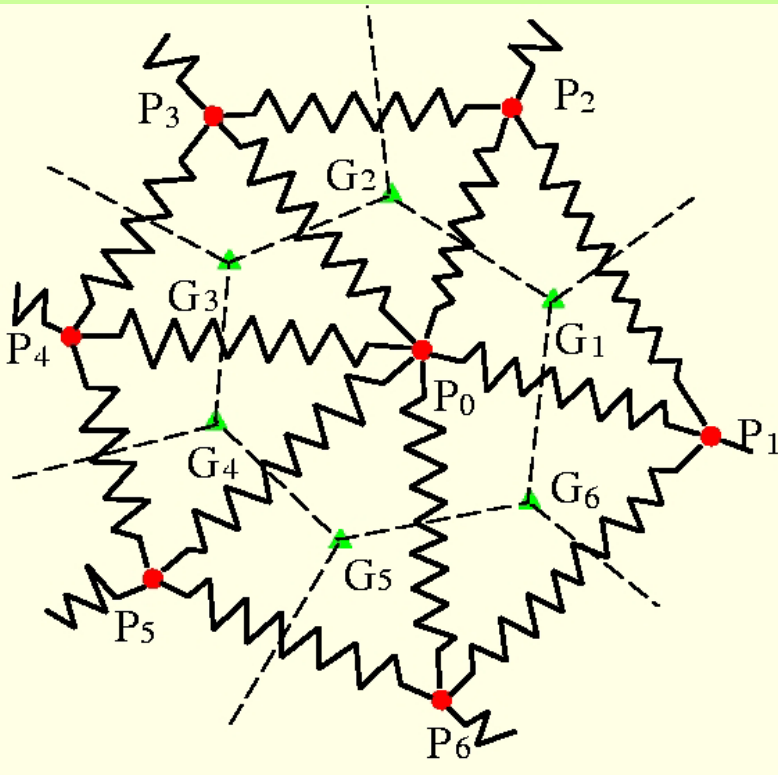
GUESS:

smoothness of CV

→ Reduction of grid noise



- Reconstruction of grid by spring dynamics
 - To reduce the grid-noise



1. **STD-grid :**
Generated by the recursive grid division.
2. **SPRING DYNAMICS :**
Connection of gridpoints by springs

$$\sum_{i=1}^6 k(d_i - \bar{d})\mathbf{e}_i - \alpha\mathbf{w}_0 = M \frac{d\mathbf{w}_0}{dt}$$

$$\mathbf{w}_0 = \frac{d\mathbf{r}_0}{dt}$$



■ SPR-grid

■ Solve the spring dynamics

→ The system calms down to the static balance

$$\sum_{i=1}^6 k(d_i - \bar{d})\mathbf{e}_i = 0$$

■ Construction of CV

- Connection of the center of triangles

■ One non-dimensional parameter β

■ Natural length of spring

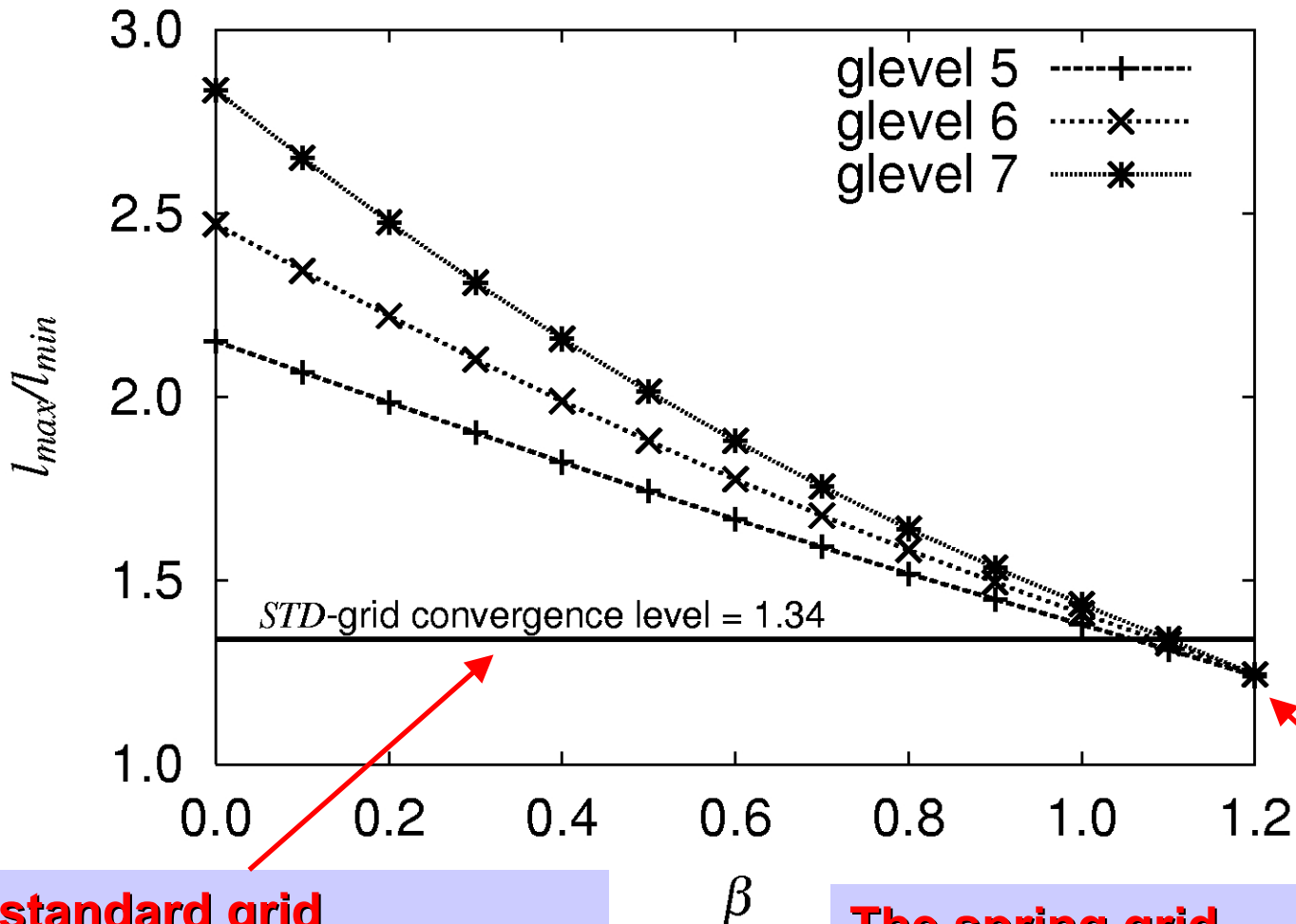
$$\bar{d} = \beta \frac{2\pi a}{10 \times 2^{l-1}}$$

- Should be tuned!



Dependency of β on homogeneity

The ratio of l_{max} / l_{min} against the parameter β



The standard grid

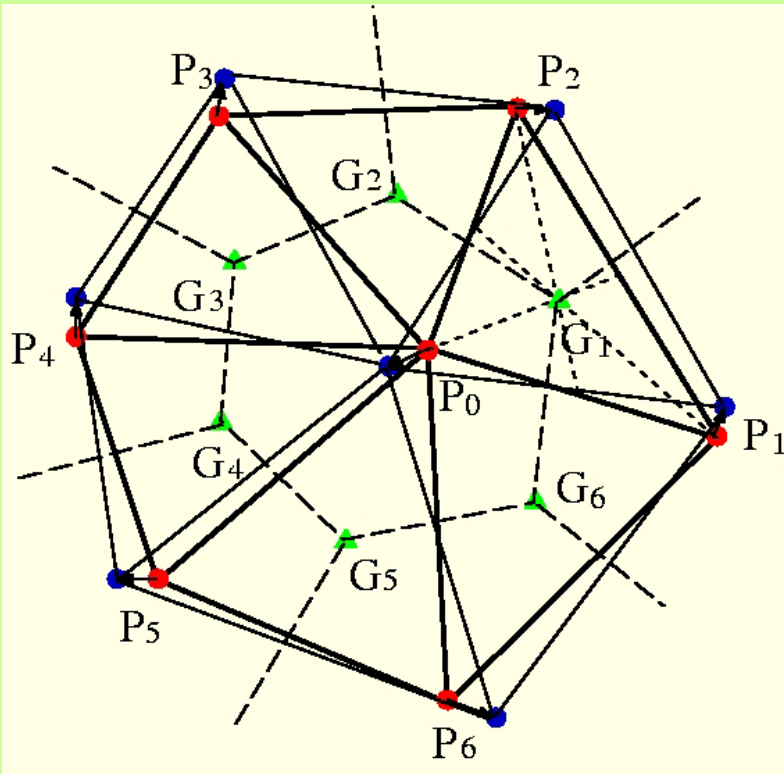
$l_{max}/l_{min} \rightarrow 1.34.$

The spring grid

l_{max}/l_{min} depends on β and glevel.
 \rightarrow If $\beta=1.2$, $l_{max}/l_{min} \rightarrow 1.24.$

■ Gravitational-Centered Relocation

■ To make the accuracy of numerical operators higher



1. **SPR-grid:**
Generated by the spring dynamics.
→ ●
2. **CV:**
Defined by connecting the GC of triangle elements.
→ ▲
3. **SPR-GC-grid:**
The grid points are moved to the GC of CV.
→ ●

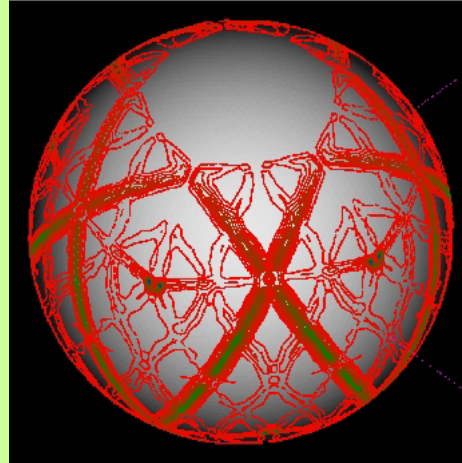
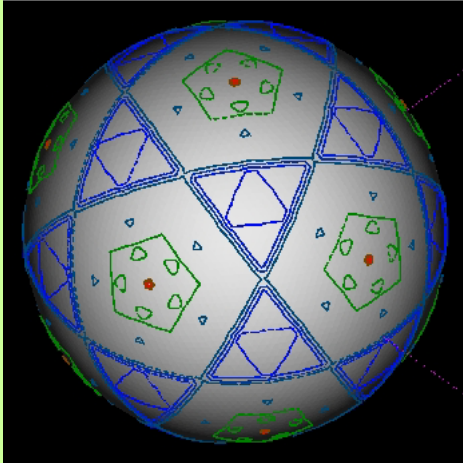
→ The 2nd order accuracy of numerical operator is perfectly guaranteed at all of grid points.



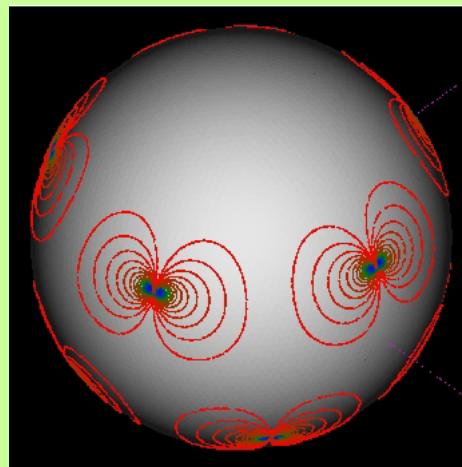
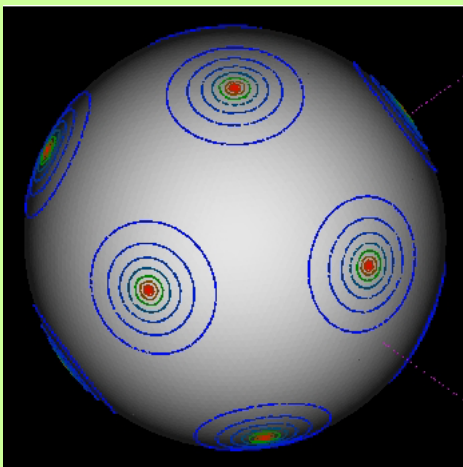
- Area of CV

- Error of divergence

STD-grid



SPR-GC-grid



■ STD-grid

■ Area of CV

- Fractal distribution due to recursive division

■ Error of divergence

- Fractal distribution error
→ Generation of grid noise

■ SPR-GC-grid

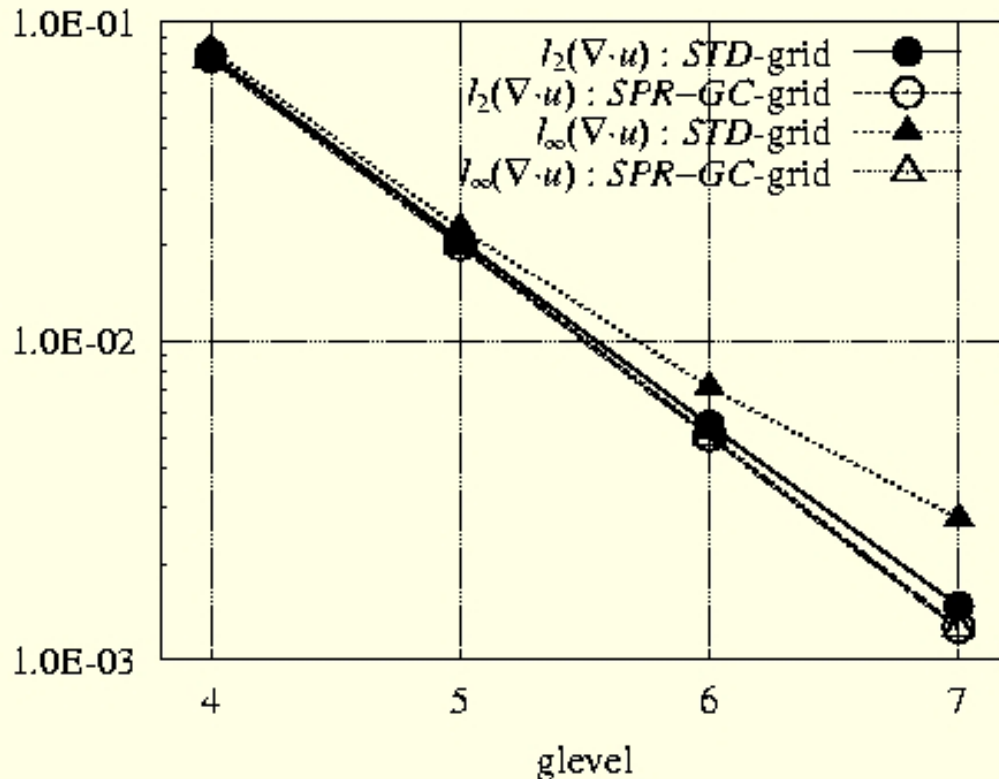
■ Area of CV

- Smooth distribution

■ Error of divergence

- Smooth distribution
→ Reduction of grid noise





■ Test function

■ Heikes & Randall(1995)

■ Error norm

■ Global error

$$l_2(x) = \frac{\{I[(x(\lambda, \theta) - x_T(\lambda, \theta))^2]\}^{1/2}}{\{I[x_T(\lambda, \theta)^2]\}^{1/2}}$$

■ Local error

$$l_\infty(x) = \frac{\max_{all \lambda, \theta} |x(\lambda, \theta) - x_T(\lambda, \theta)|}{\max_{all \lambda, \theta} |x_T(\lambda, \theta)|}$$

	STD-grid	SPR-GC-grid
L_2 norm	Almost 2nd-order(●)	Perfect 2nd-order(○)
L_inf norm	Not 2nd order(▲)	Perfect 2nd-order(△)



■ Shallow water equations

■ Vector invariant form

$$\frac{\partial \mathbf{v}}{\partial t} + (\hat{\mathbf{k}} \cdot \nabla \times \mathbf{v} + f) \hat{\mathbf{k}} \times \mathbf{v} = -\nabla \left(gh + \frac{\mathbf{v} \cdot \mathbf{v}}{2} \right) \quad (1)$$

$$\frac{\partial h^*}{\partial t} + \nabla \cdot (h^* \mathbf{v}) = 0 \quad (2)$$

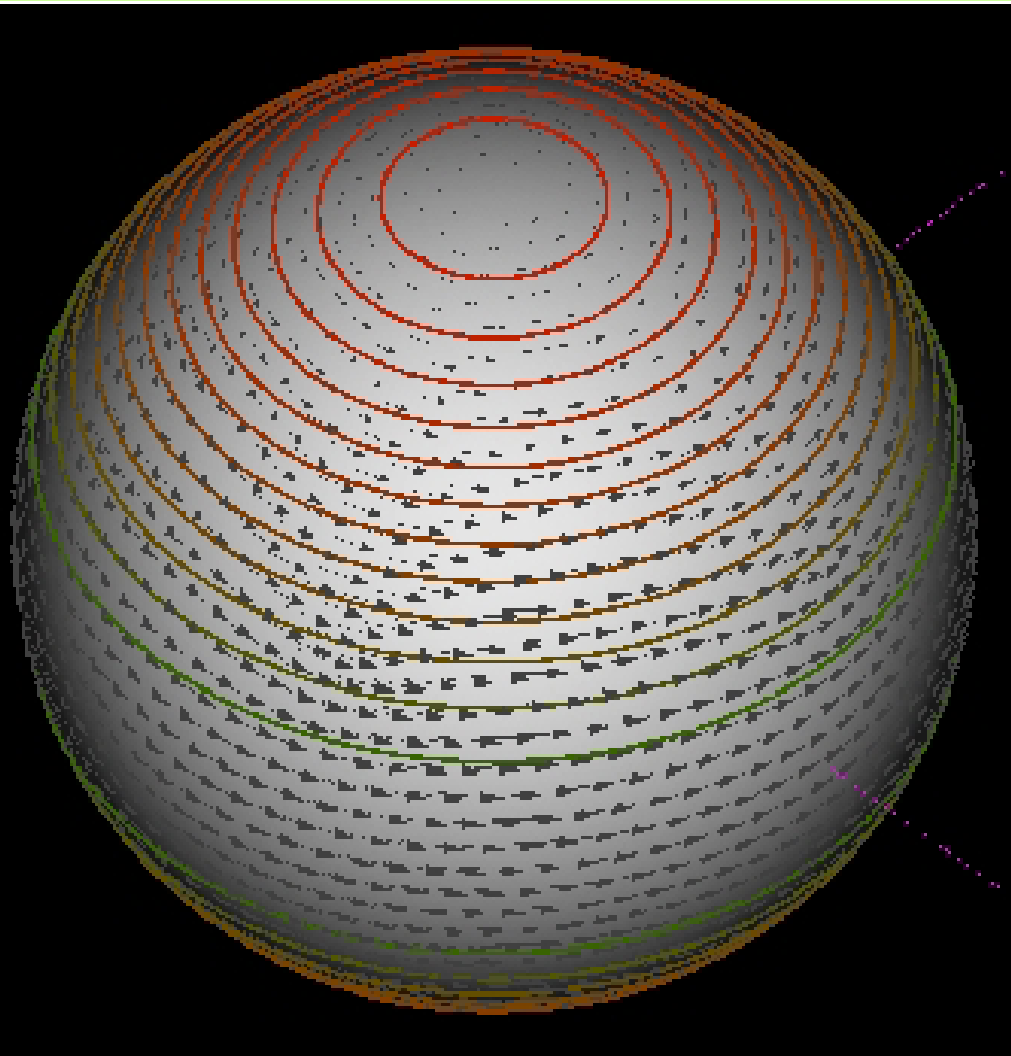
where $h = h^* + h_s$

■ A Standard Test Case

■ Williamson et al. (1992, JCP)

- **TEST CASE2**
 - Solid body rotation test
- **TEST CASE5**
 - Unsteady, nonlinear but deterministic test with mountain





■ Test configuration

■ Initial condition

- Solid body rotation
- Geostrophic balance

■ Purpose

- How does the model maintain the initial state?

■ Integration time

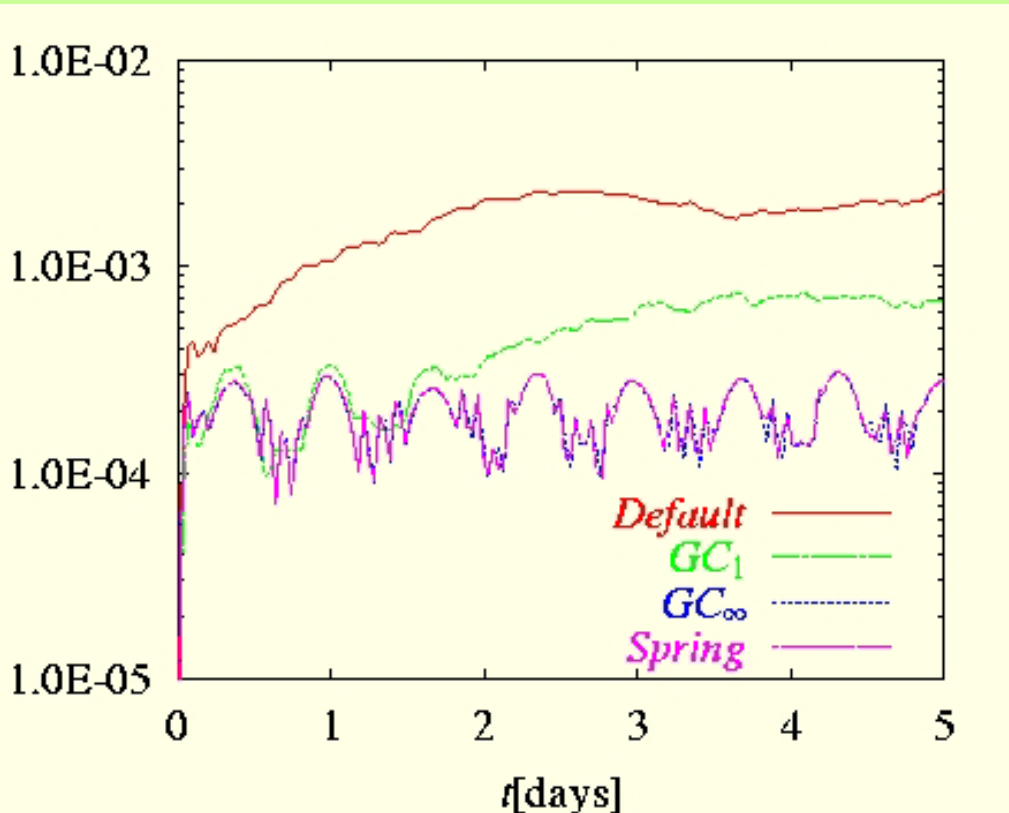
- 5 days

■ Monitor

■ Time evolution of L_∞ norm of surface height



Time evolution l_{∞} norm



Numerical condition

- Resolution : glevel-5
- Integration : 5day
- numerical diffusion : none

■ STD-grid (---)

- No modification of grid

- Large error from the initial stage

■ STD-GC-grid (---)

- Only GCR modification

- Small error just in 1 day

- Large error from 2 day

→ Grid-noise

■ SPR-GC-grid (---)

- Spring dyn & GCR

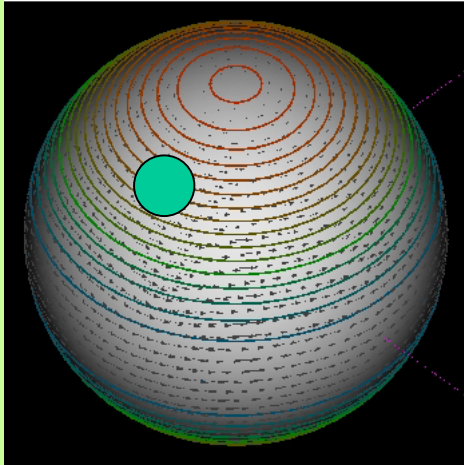
- Small error during 5 days

→ No grid-noise

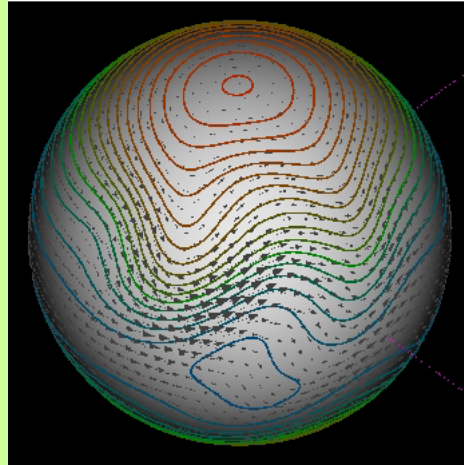


Result : glevel5 SPR-GC grid without viscosity

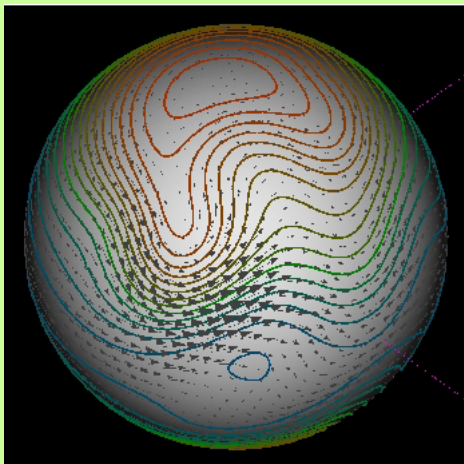
(0) t=0 day



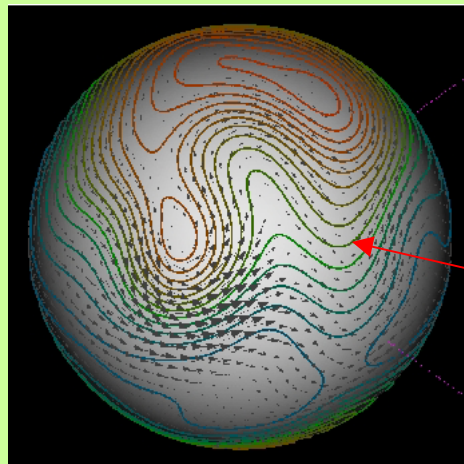
(1) t=5 day



(2) t=10 day



(3) t=15 day



■ Test Configuration

■ Initial condition

- Solid body rotation
- Mountain at the mid-latitude

■ Integration

- 15 days

■ Purpose

- Check the conservation

Total energy

$$TE = \frac{1}{2} h^* \mathbf{v} \cdot \mathbf{v} + \frac{1}{2} g (h^2 - h_s^2)$$

Potential enstrophy

$$PENS = \frac{1}{2h^*} (\zeta + f)^2$$

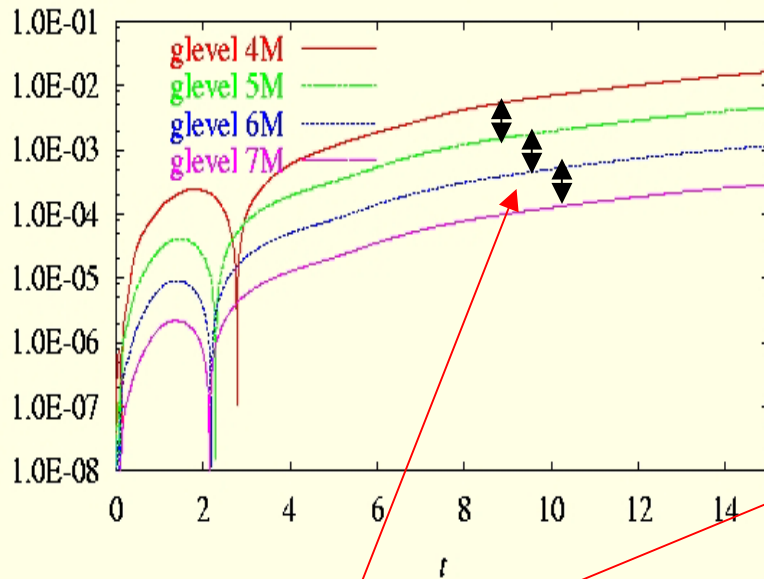
No grid noise



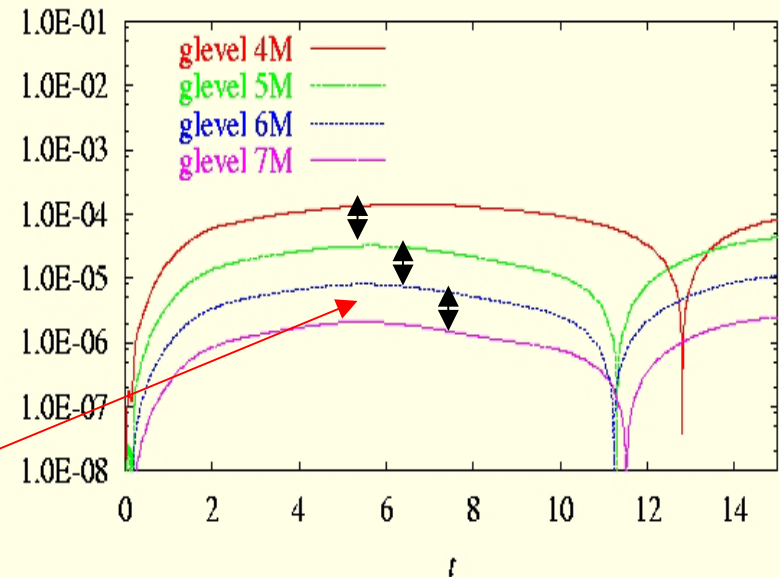
■ Grid refinement result (SPR-GC grid)

- Resolution : glevel-4,5,6,7
- Numrical diffusion : NONE

Conservation of total energy $(E_{TE0})/TE01$



Conservation of potential enstrohpy $(NS01)$



**Error : reduction by a factor of 4
→ in the 2nd order**





Nonhydrostatic framework





■ Governing equation

■ Full compressible system

- Acoustic wave → Planetary wave

■ Flux form

- Finite Volume Method
- Conservation of mass and energy

■ Deep atmosphere

- Including all metrics terms and Coriolis terms

■ Solver

■ Split explicit method

- Slow mode : Large time step
- Fast mode : small time step

■ HEVI (Horizontal Explicit & Vertical Implicit)

- 1D-Helmholtz equation



← L.H.S. : FAST MODE → ← R.H.S. : SLOW MODE →

$$\frac{\partial}{\partial t} R + \nabla_h \cdot \frac{\mathbf{V}_h}{\gamma} + \frac{\partial}{\partial \xi} \left(\frac{W}{G^{1/2}} + \mathbf{G}^3 \cdot \frac{\mathbf{V}_h}{\gamma} \right) = 0 \quad (1)$$

$$\frac{\partial}{\partial t} \mathbf{V}_h + \nabla_h \frac{P}{\gamma} + \frac{\partial}{\partial \xi} \left(\mathbf{G}^3 \frac{P}{\gamma} \right) = \mathbf{ADV}_h + \mathbf{F}_{Coriolis} \quad (2)$$

$$\frac{\partial}{\partial t} W + \gamma^2 \frac{\partial}{\partial \xi} \left(\frac{P}{G^{1/2} \gamma^2} \right) + Rg = ADV_z + F_{Coriolis} \quad (3)$$

$$\begin{aligned} & \frac{\partial}{\partial t} E + \nabla_h \cdot \left(h \frac{\mathbf{V}_h}{\gamma} \right) + \frac{\partial}{\partial \xi} \left[h \left(\frac{W}{G^{1/2}} + \mathbf{G}^3 \cdot \frac{\mathbf{V}_h}{\gamma} \right) \right] \\ & - \frac{\mathbf{V}_h}{R} \cdot \left[\nabla_h \frac{P}{\gamma} + \frac{\partial}{\partial \xi} \left(\mathbf{G}^3 \frac{P}{\gamma} \right) \right] - \frac{W}{R} \gamma^2 \frac{\partial}{\partial \xi} \left(\frac{P}{G^{1/2} \gamma^2} \right) + Wg = Q_{heat} \end{aligned} \quad (4)$$

■ Prognostic variables

- **density** $R = \gamma^2 G^{1/2} \rho$
- **horizontal momentum** $\mathbf{V}_h = \gamma^2 G^{1/2} \rho \mathbf{v}_h$
- **vertical momentum** $W = \gamma^2 G^{1/2} \rho w$
- **internal energy** $E = \gamma^2 G^{1/2} \rho e_{in}$

■ Metrics

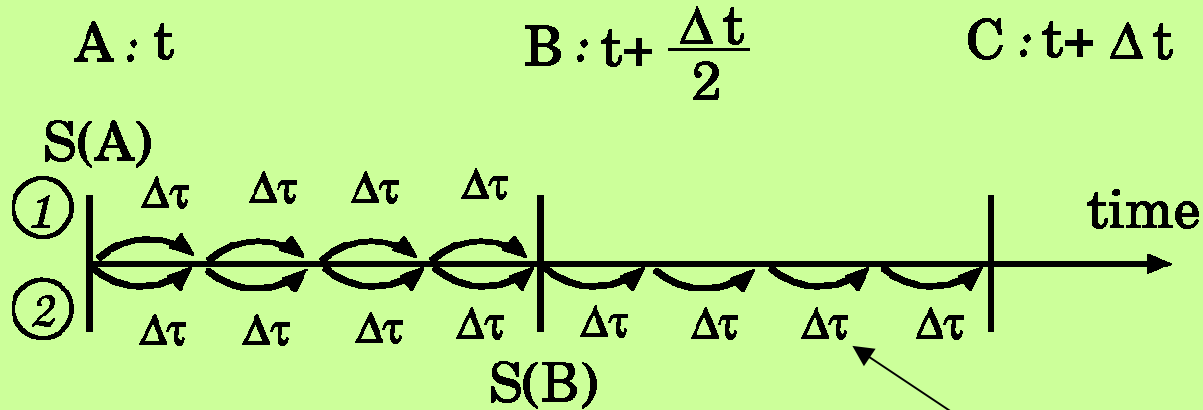
$$G^{1/2} = \left(\frac{\partial z}{\partial \xi} \right)_{x,y}$$

$$\mathbf{G}^3 = (\nabla_h \xi)_z$$

$$\xi = \frac{H(z - z_s)}{H - z_s}$$



Temporal Scheme (RK2)



Assumption : the variable at $t=A$ is known.

➤ Obtain the slow mode tendency $S(A)$.

1. **1st step :**

Integration of the prog. var. by using $S(A)$ from A to B .

➤ Obtain the tentative values at $t=B$.

➤ Obtain the slow mode tendency $S(B)$ at $t=B$.

2. **2nd step :**

Returning to A , Integration of the prog.var. from A to C by using $S(B)$.

→ **Obtain the variables at $t=C$**

HEVI solver



In small step integration, there are 3 steps:

1. Horizontal Explicit Step

- Update of horizontal momentum

2. Vertical Implicit Step

- Updates of vertical momentum and density.

3. Energy Correction Step

- Update of energy

} **HEVI**

■ Horizontal Explicit Step

- Horizontal momentum is updated explicitly by

$$\mathbf{V}_h^{t+(n+1)\Delta\tau} = \mathbf{V}_h^{t+n\Delta\tau} + \Delta\tau \left[\left(-\nabla_h \frac{P}{\gamma} - \frac{\partial}{\partial \xi} \left(\mathbf{G}^3 \frac{P}{\gamma} \right) \right)^{t+n\Delta\tau} + \left(\frac{\partial \mathbf{V}_h}{\partial t} \right)_{\text{slow mode}}^{[t, \text{ or } t+\Delta t/2]} \right]$$

Fast mode

**Slow mode :
given**



■ Vertical Implicit Step

- The equations of R,W, and E can be written as:

$$\frac{R^{t+(n+1)\Delta\tau} - R^{t+n\Delta\tau}}{\Delta\tau} + \frac{\partial}{\partial\xi} \left(\frac{W^{t+(n+1)\Delta\tau}}{G^{1/2}} \right) = G_R \quad (6)$$

$$\frac{W^{t+(n+1)\Delta\tau} - W^{t+n\Delta\tau}}{\Delta\tau} + \gamma^2 \frac{\partial}{\partial\xi} \left(\frac{P^{t+(n+1)\Delta\tau}}{G^{1/2}\gamma^2} \right) + R^{t+(n+1)\Delta\tau} g = G_z \quad (7)$$

$$\frac{P^{t+(n+1)\Delta\tau} - P^{t+n\Delta\tau}}{\Delta\tau} + \frac{\partial}{\partial\xi} \left[\left(\frac{W^{t+(n+1)\Delta\tau}}{G^{1/2}} \right) c_s^{2t+n\Delta\tau} \right] + \frac{R_d}{C_V} W^{t+(n+1)\Delta\tau} \tilde{g} = \frac{R_d}{C_V} G_E \quad (8)$$

- Coupling Eqs.(6), (7), and (8), we can obtain the 1D-Helmholtz equation for W :

$$\frac{W^{t+(n+1)\Delta\tau}}{\gamma^2} - \frac{\partial}{\partial\xi} \left[\frac{1}{G^{1/2}\gamma^2} \frac{\partial}{\partial\xi} \left(\Delta\tau^2 c_s^{2t+n\Delta\tau} \frac{W^{t+(n+1)\Delta\tau}}{G^{1/2}} \right) \right] - \left[\frac{\partial}{\partial\xi} \left(\Delta\tau^2 \frac{R_d}{C_V} \tilde{g} \frac{W^{t+(n+1)\Delta\tau}}{G^{1/2}\gamma^2} \right) \right] + \Delta\tau^2 \frac{g}{\gamma^2} \frac{\partial}{\partial\xi} \left(\frac{W^{t+(n+1)\Delta\tau}}{G^{1/2}} \right) = \text{R.H.S. (source term)} \quad (9)$$

- Eq.(9) → W
- Eq.(6) → R
- Eq.(8) → E



■ Energy Correction Step

(Total eng.) = (Internal eng.) + (Kinetic eng.) + (Potential eng.)

- **We consider the equation of total energy**

$$\frac{\partial}{\partial t} E_{total} + \nabla_h \cdot \left[(h + k + \Phi) \frac{\mathbf{V}_h}{\gamma} \right] + \frac{\partial}{\partial \xi} \left[(h + k + \Phi) \left(\frac{W}{G^{1/2}} + \mathbf{G}^3 \cdot \frac{\mathbf{V}_h}{\gamma} \right) \right] = 0 \quad (10)$$

where $E_{total} = \rho \gamma^2 G^{1/2} (e_{in} + k + \Phi)$

- **Additionally, Eq.(10) is solved as**

$$E_{total}^{t+(n+1)\Delta\tau} = E_{total}^{t+n\Delta\tau} - \Delta\tau \left[\nabla_h \cdot \left[(h + k + \Phi) \frac{\mathbf{V}_h}{\gamma} \right] + \frac{\partial}{\partial \xi} \left[(h + k + \Phi) \left(\frac{W}{G^{1/2}} + \mathbf{G}^3 \cdot \frac{\mathbf{V}_h}{\gamma} \right) \right] \right]^{t+(n+1)\Delta\tau}$$

– **Written by a flux form.**

- **The kinetic energy and potential energy:**
 → **known by previous step.**
- **Recalculate the internal energy:**

$$E^{t+(n+1)\Delta\tau} = E_{total}^{t+(n+1)\Delta\tau} - \rho^{t+(n+1)\Delta\tau} \gamma^2 G^{1/2} (k^{t+(n+1)\Delta\tau} + \Phi)$$



■ Large step tendency has 2 main parts:

1. Coriolis term

- Formulated straightforward.

2. Advection term

- We should take some care to this term because of curvature of the earth

■ Advection of momentum

■ The advection term of V_h and W is calculated as follows.

1. Construct the 3-dimensional momentum \mathbf{V} using \mathbf{V}_h and W .
2. Express this vector as 3 components as (V_1, V_2, V_3) in a fixed coordinate.

➤ **These components are scalars.**

3. Obtain a vector which contains 3 divergences as its components.

$$\rightarrow (\nabla \cdot v_1 \mathbf{V}, \nabla \cdot v_2 \mathbf{V}, \nabla \cdot v_3 \mathbf{V}) \quad \text{where } v_i = V_i / (G^{1/2} \gamma^2 \rho)$$

4. Split again to a horizontal vector and a vertical components.

$$\rightarrow ADV_h, ADV_z$$



Test results of 3D-model



■ Test configuration

■ Radiation

- We use a simple radiation as Newtonian Cooling of temperature field :

$$\frac{dT}{dt} = \dots - k_T(\phi, \sigma)(T - T_{eq}) \quad : \quad k_T = k_a + (k_s - k_a) \max\left(0, \frac{\sigma - \sigma_b}{1 - \sigma_b}\right) \cos^4 \phi$$

where $\sigma_b = 0.7$, $k_a = 1/40$ [/day], $k_s = 1/4$ [/day]

- Equilibrium temperature is zonally symmetric as:

$$T_{eq} = \max\left[200\text{K}, \left[315\text{K} - (\Delta T)_y \sin^2 \phi - (\Delta \theta)_z \log\left(\frac{p}{p_0}\right) \cos^2 \phi\right] \left(\frac{p}{p_0}\right)^\kappa\right]$$

where $(\Delta T)_y = 60\text{K}$, $(\Delta \theta)_z = 10\text{K}$

■ Surface friction

- Surface friction is imposed in the lower atmosphere as a Rayleigh damping :

$$\frac{dV}{dt} = \dots - k_V(\sigma)(T - T_{eq}) \quad : \quad k_V = k_f \max\left(0, \frac{\sigma - \sigma_b}{1 - \sigma_b}\right)$$

- where $k_f = 1/1$ [/day]



■ Objective

- After 1200 days integration, the climatology in the 1000 days are checked.
- The results obtained are compared with other models.

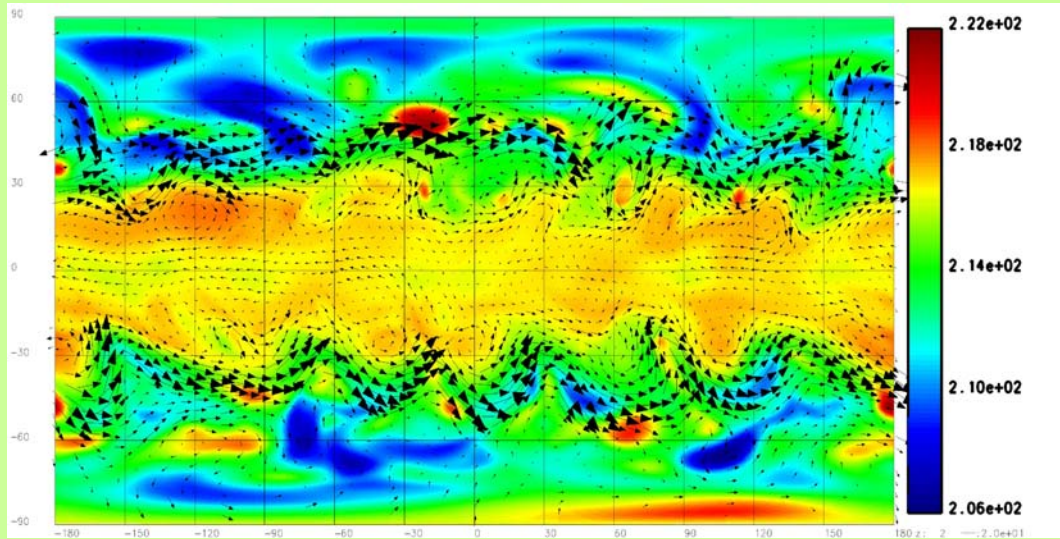
■ Model used

- AFES(AGCM For Earth Simulator)
 - Based on the CCSR/NIES spectral model.
 - T319L32(resolvable scale = 120km on the equator).
- NICAM(Nonhydrostatic Icosahedral Atmospheric Model)
 - Glevel-7L32(grid intv. = 60km on the equator)

Resolvable scale (T319 \leftrightarrow Glevel-7) : almost same
Hyper diffusion (4th order) : exactly same

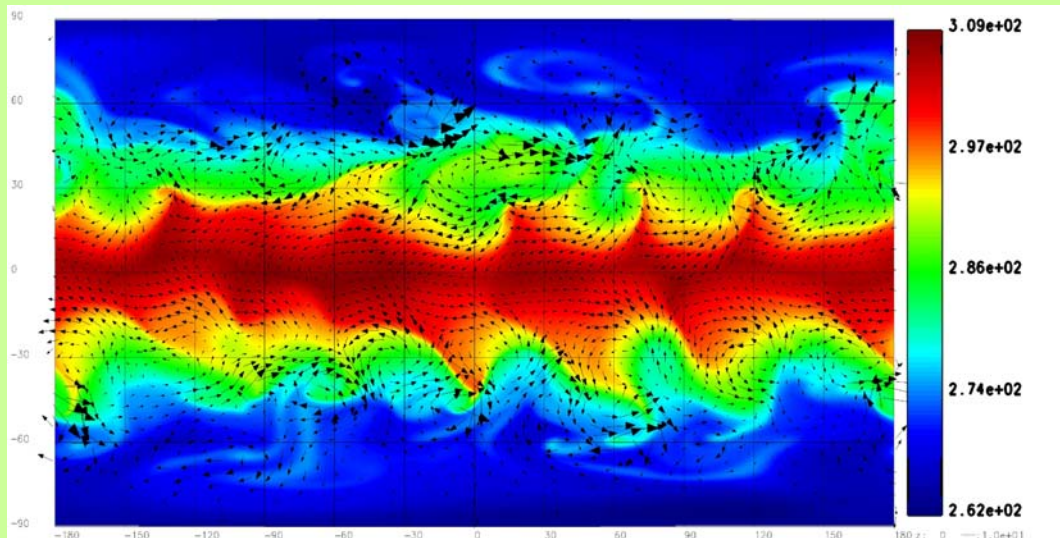


■ Snapshot results (T and v_h fields after 1200 days)



■ Upper atmosphere ($z=10.5\text{km}$)

The westerly jet in the mid-latitude and the baroclinic instability is well simulated



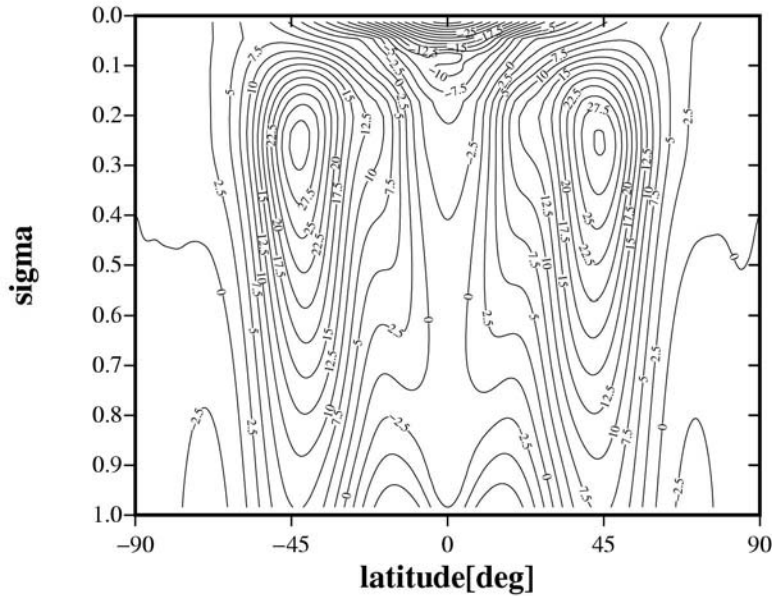
■ Lower atmosphere ($z=0.5\text{km}$)

The easterly wind near the equatorial region is well simulated.

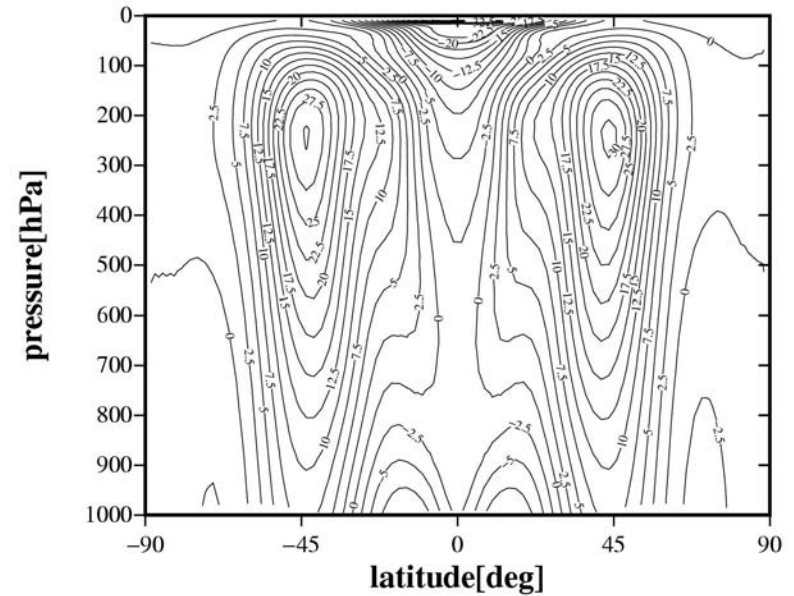


■ Zonal mean of zonal wind

AFES(T319L32)



NICAM(glevel7-L32)



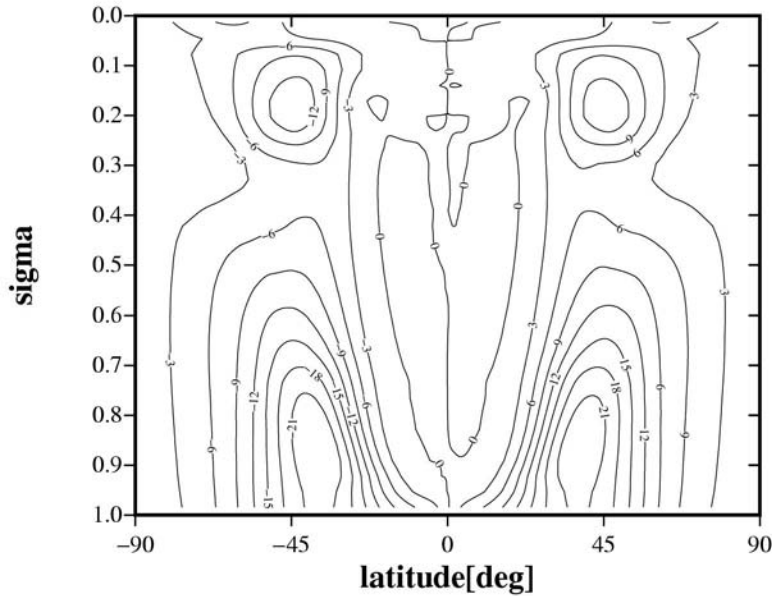
■ No significant difference

- The location & intensity of jet is almost same.

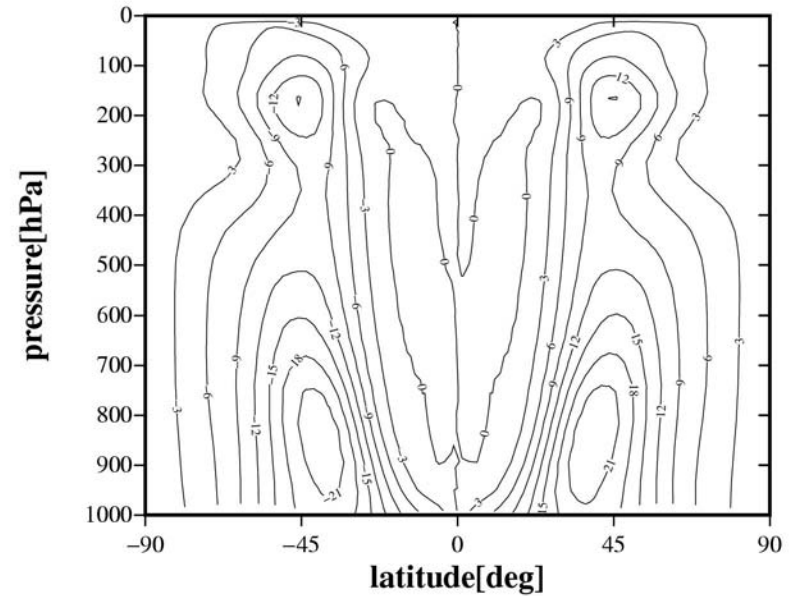


■ Zonal mean of eddy heat flux ($v'T'$)

AFES(T319L32)

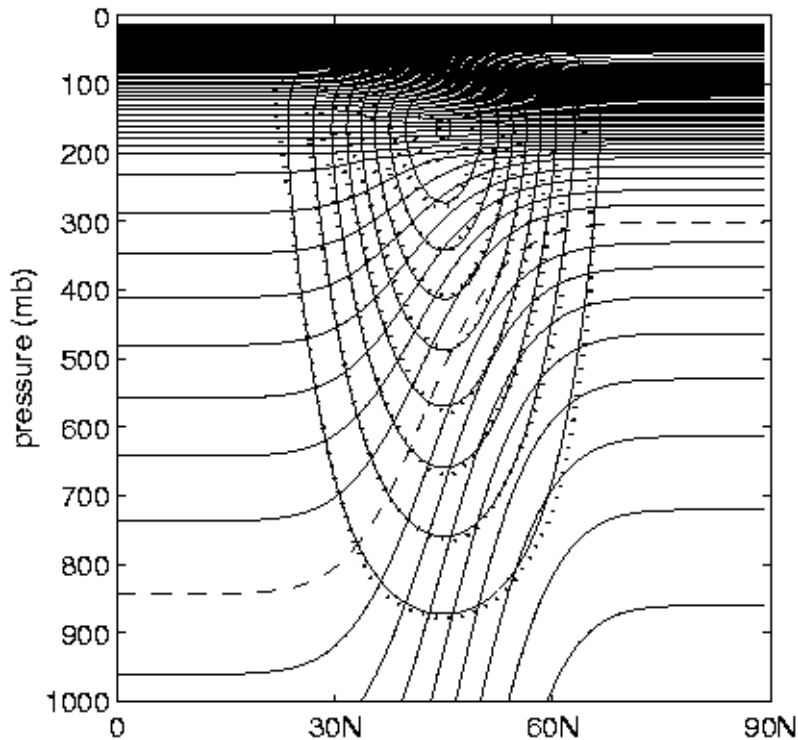


NICAM(glevel7-L32)



- Almost same intensity for both models
- Acceptable difference!





Initial balance state in the northern hemisphere. Potential temperature & zonal wind profile

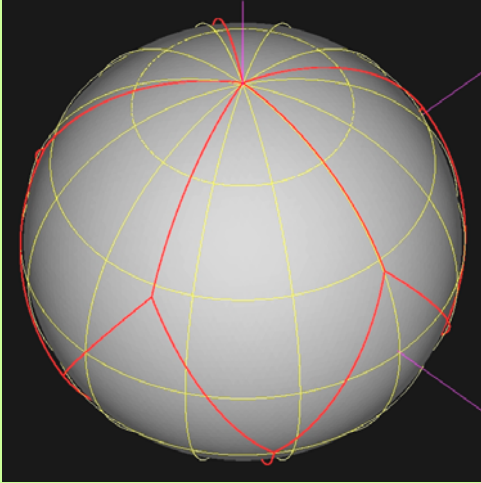
■ Test Configuration

(Polvani et al, submitted to MWR)

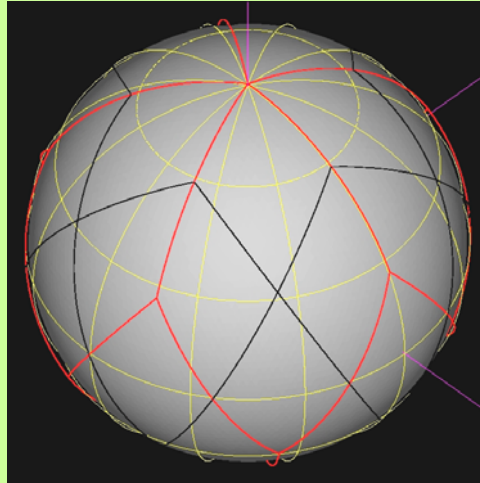
- Zonal jet in the northern hemisphere
→ max speed : 50 [m/s]
- Thermal wind balance in the horizontal
- Hydrostatic balance in the vertical.
- A thermal disturbance of cosine bell in the mid-latitude.



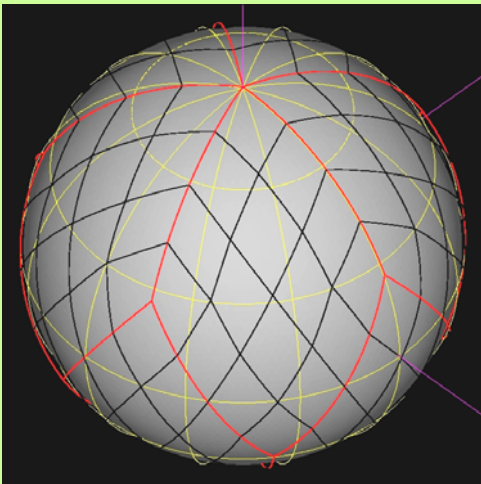
(0) region division level 0



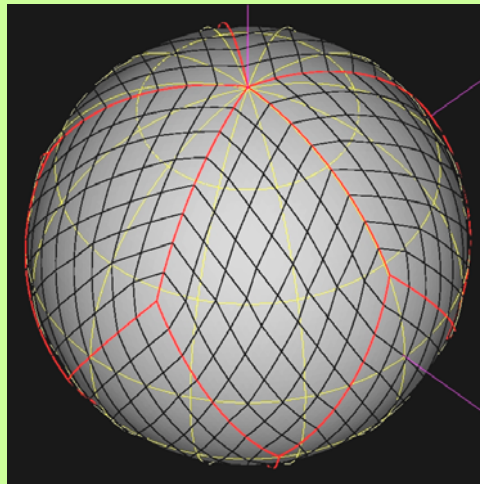
(1) region division level 1



(2) region division level 2



(3) region division level 3

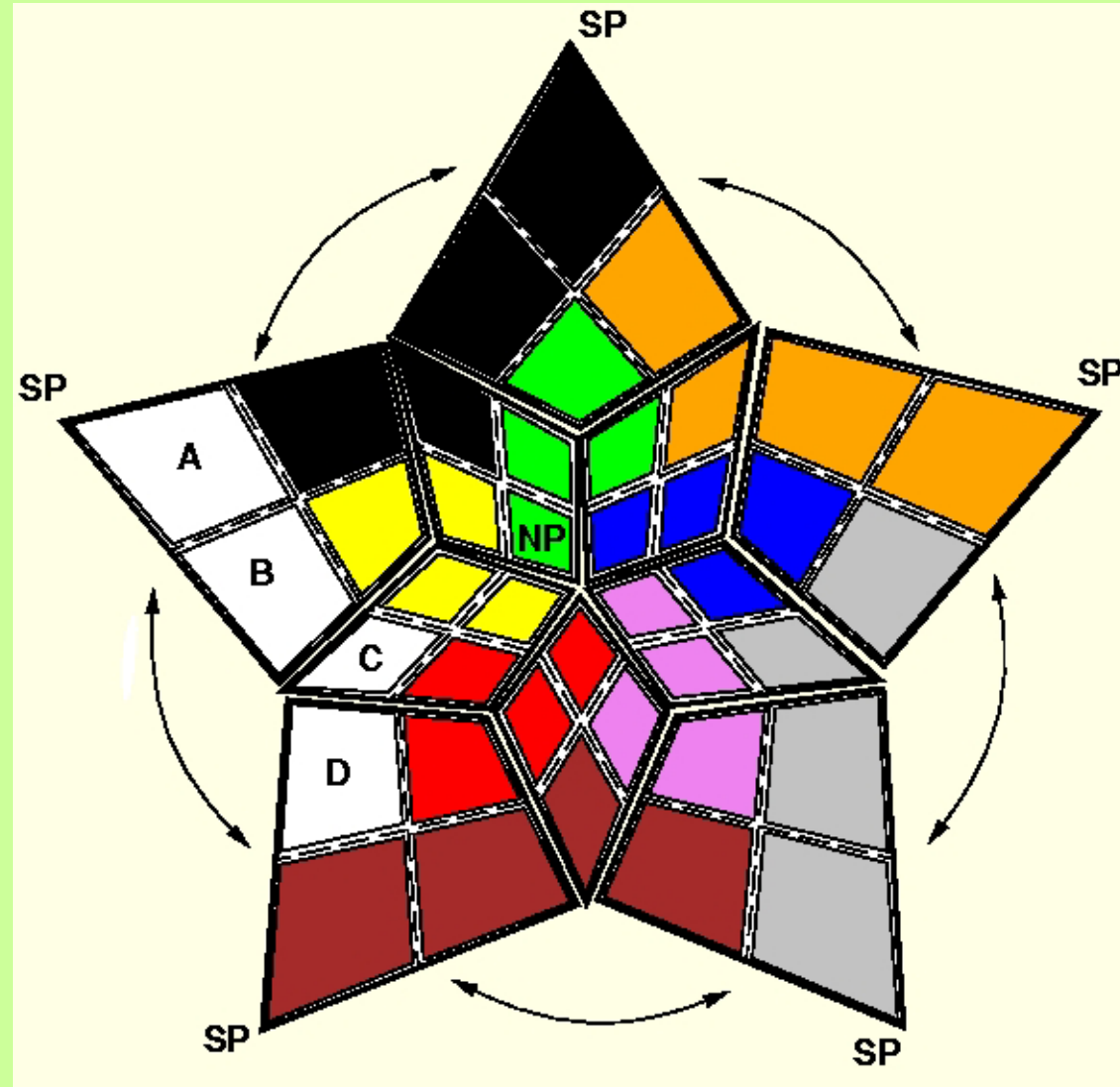


■ Domain decomposition

1. By connecting two neighboring icosahedral triangles, 10 rectangles are constructed. (rlevel-0)
2. For each of rectangles, 4 sub-rectangles are generated by connecting the diagonal mid-points. (rlevel-1)
3. The process is repeated. (rlevel-n)



Load balancing



■ Example (rlevel-1)

- # of region : 40
- # of process : 10
- **Situation:**
 - Polar region:
Less computation
 - Equatorial region:
much computation

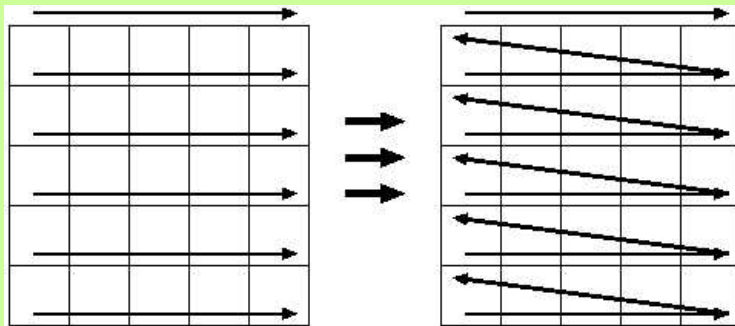
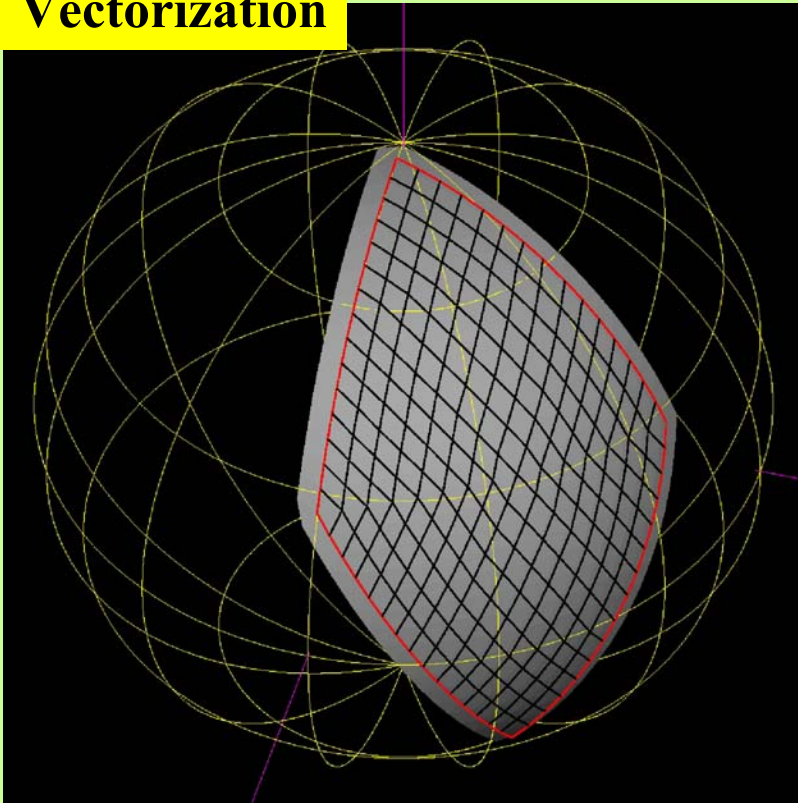
■ Each process

- manage same color regions
- Cover from the polar region and equatorial region.

Avoid the load imbalance



Vectorization



- Structure in one region
 - Icosahedral grid
 - Unstructured grid?
 - Treatment as structured grid
 - Fortran 2D array
 - vectorized efficiently!

- 2D array → 1D array
 - Higher vector operation length



■ Computational performance

■ Depend on the many things

- Computer architecture, degree of code tuning.....

■ Rough comparison between GPM & SM

- AFES as one of spectral models
- NICAM as one of gridpoint models
- Both models are well tuned on the Earth Simulator.

■ Performance on the Earth Simulator

■ Earth Simulator

- Massively parallel super-computer based on NEC SX-6 architecture.
 - 640 computational nodes.
 - 8 vector-processors in each of nodes.
 - Peak performance of 1CPU : 8GFLOPS
 - Total peak performance : $8 \times 8 \times 640 = 40\text{TFLOPS}$

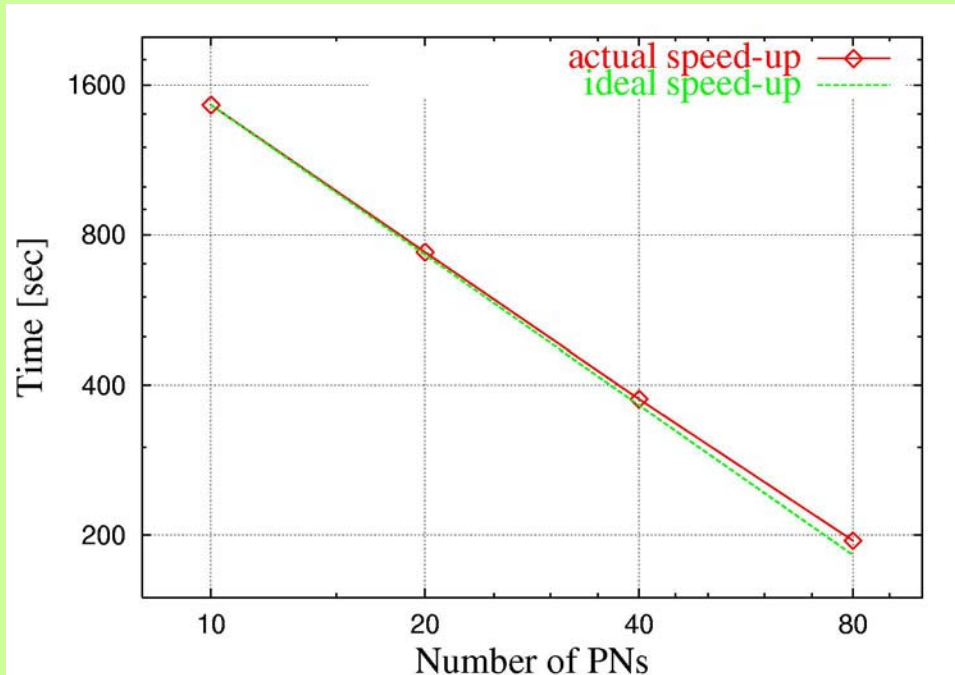


■ Target simulations for the measurement

- 1 day simulation of Held & Suarez dynamical core experiment



■ Scalability of our model (NICAM)



Configuration

- Horizontal resolution : glevel-8
- Vertical layers : 100



Fixed

- The used computer nodes increases from 10 to 80.

Results

Green : ideal speed-up line

Red : actual speed-up line

→ good scalability!



■ Performance against the horizontal resolution

The elapse time should increase by a factor of 2.

g level (grid intv.)	Number of PNs (peak performance)	Elapse Time [sec]	Average Time [msec]	GFLOPS (ratio to peak[%])
6 (120km)	5 (320GFLOPS)	48.6	169	140 (43.8)
7 (60km)	20 (1280GFLOPS)	97.4	169	558 (43.6)
8 (30km)	80 (5120GFLOPS)	195	169	2229 (43.5)
9 (15km)	320 (20480GFLOPS)	390	169	8916

Configuration

As the glevel increases,

of gridpoints : X 4

of CPUs : X 4

Time intv. : 1/2

Results

Actually, the elapse time increases by a factor of 2.



■ Comparison of performance between SM & GPM

■ Discussion point

- Which is computationally efficient?
 - Computer performance depends on many things.
 - This attempt is just one example.

■ Condition

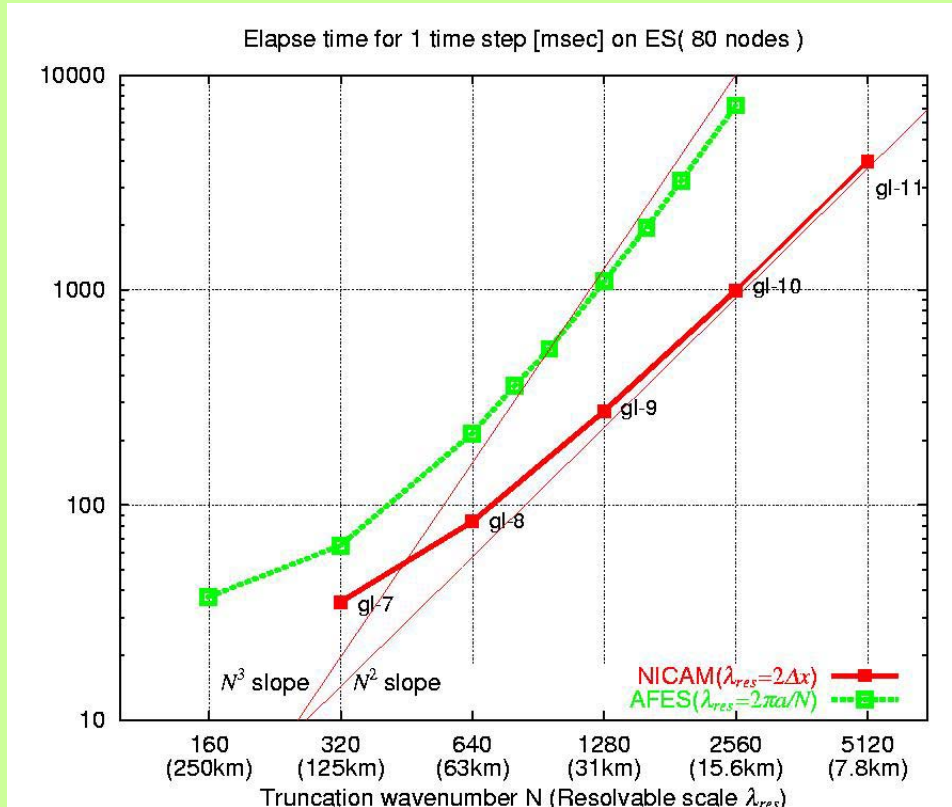
- Vertical layer : 32
- Horizontal resolution : T160 → T2560 (AFES)
GI-6 → GI-10 (NICAM)
- 80 nodes of ES
- Only dynamical core (without any physical processes)

■ Estimation method

- There are two factors for estimations.
 - Elapse time of 1 time step
 - Available time step Δt
- By considering two factors,
Estimation of elapse time of 1 day simulation.



■ Elapse time of 1step for NICAM and AFES



■ A F E S (green line)

Elapse time increases in the sense $O(n^3)$.

→ Legendre transformation

■ N I C A M (red line)

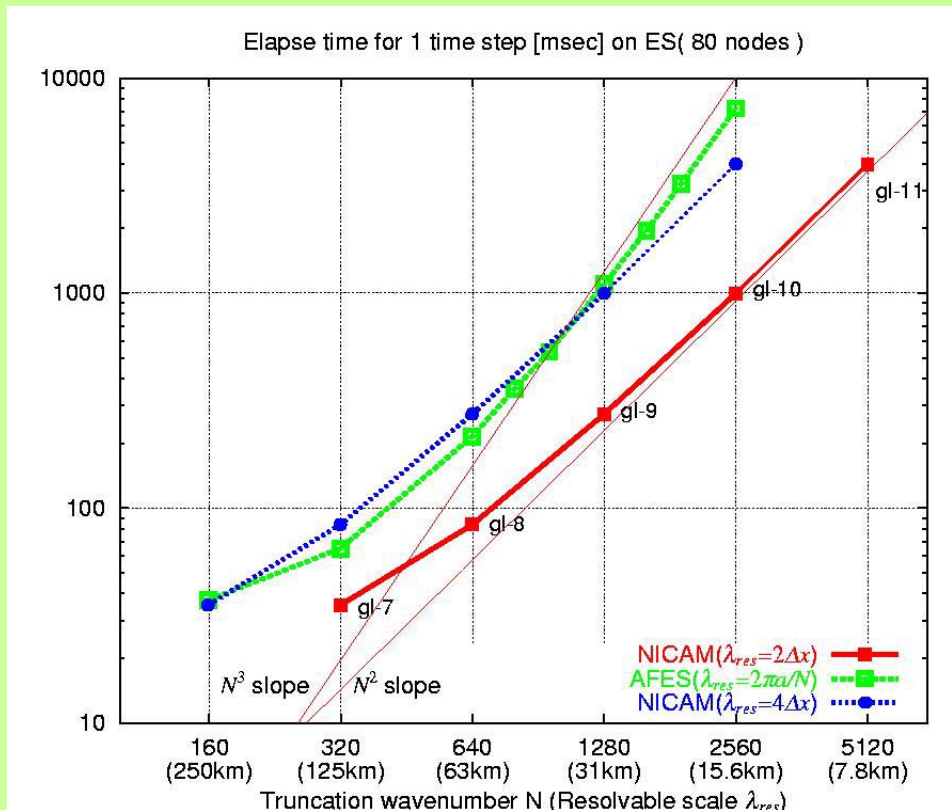
Elapse time increases in the sense $O(n^2)$.

■ In all resolutions, NICAM is faster than AFES.

**In gridpoint models, 2 grid-scale is the resolvable scale?
→ grid noise?**



■ To consider 4-grid scale as a resolvable scale.



■ Resolution correspondance

glevel-7 → T160

glevel-8 → T320

→ **The red line** shifts to
the blue line.

■ Cross point

resolvable scale : 30km

**Even in this consideration,
GPM will be faster than SM in the 30km resolvable scale or less.**



■ Available time step Δt & 1 day simulation time

<u>NICAM</u>	<u>gl7</u>	<u>gl8</u>	<u>gl9</u>	<u>gl10</u>	<u>gl11</u>
Δt	<u>450</u>	<u>225</u>	<u>113</u>	<u>57</u>	<u>29</u>
<u>1day time</u>	<u>6.70</u>	<u>32.1</u>	<u>210</u>	<u>1519</u>	<u>12200</u>

<u>AFES</u>	<u>T159</u>	<u>T319</u>	<u>T639</u>	<u>T1279</u>	<u>T2559</u>
Δt	<u>400</u>	<u>200</u>	<u>100</u>	<u>50</u>	<u>25</u>
<u>1day time</u>	<u>8.02</u>	<u>27.9</u>	<u>184</u>	<u>1884</u>	<u>24930</u>

- Available Δt : comparable between two model.
- By considering the 1step time measuremet,
**1 day simulation time for GPM
 is much reduced in the higer resolution
 than T1000 for SM.**





■ Problem in the early development stage

■ Dfficult to do trial and error in 3.5km grid

- Limitation of computer resource

■ Solution

■ Reduce the earth radius

- e.g. $R=6400\text{km} \rightarrow 640\text{km}$

■ Use a stretched grid

- Make the gridpoints clustered in a region intersted by an appropriate transformation function
 - Schmidt transformation
 - » Isotropic transformation

We can fast develop the cloud resolving model by the combination of these strategies.

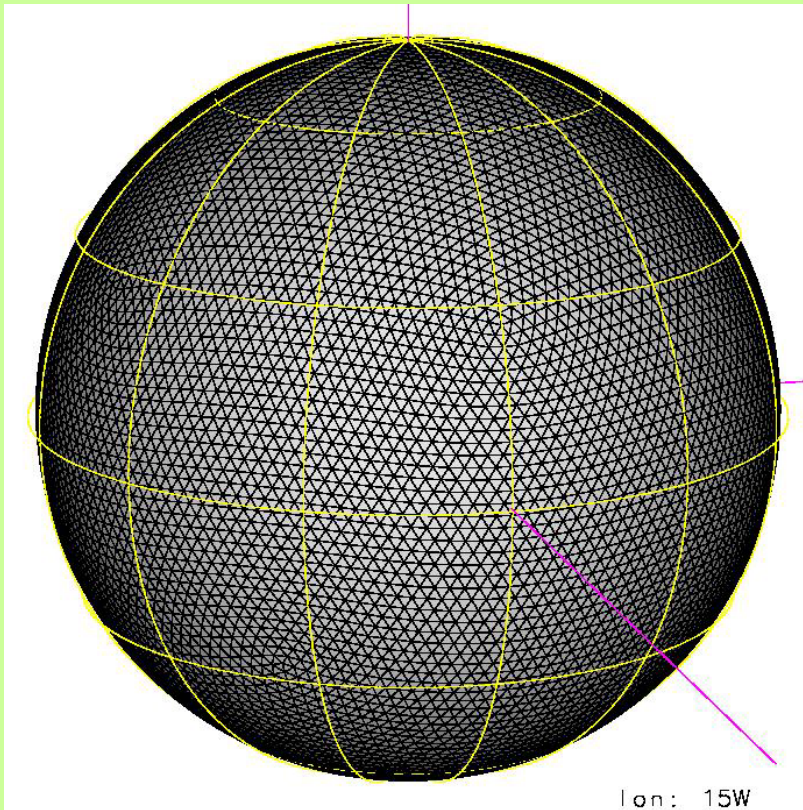


Example of stretched grid

■ Default grid : glevel-6

■ 120km grid intv.

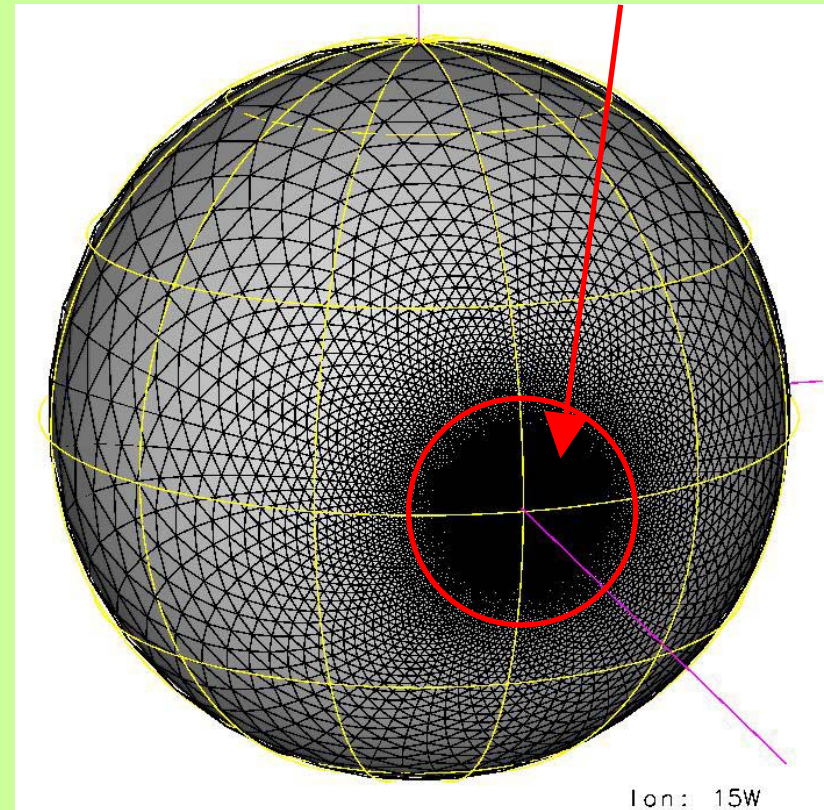
- Homogenous



■ Stretched grid

■ After the transformation

- Grid interval :
– 120km → **12km**

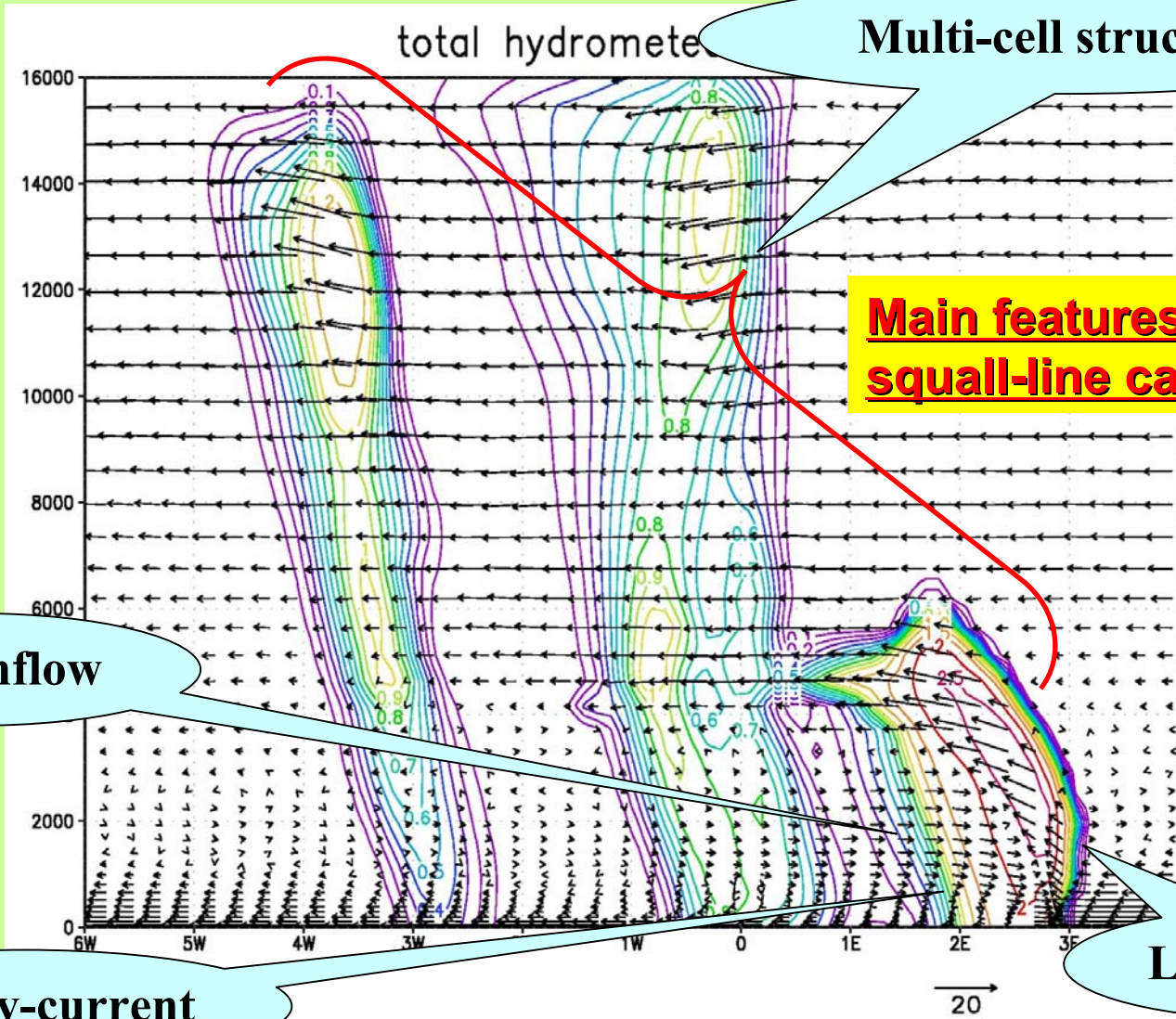


Reduction of earth radius : 1/10
1.2km grid interval



Squall-line-experiment by stretched grid

Total hydrometeor[g/kg] and velocity field



Multi-cell structure

Main features of tropical squall-line can be captured

Rear-inflow

Gravity-current

Leading edge



- We have developed a new dynamical core based on non-hydrostatic system using the icosahedral grid.
 - In this scheme, the mass and total energy are numerically conserved for the long time climate simulations.
- We performed many test cases such as the Held & Suarez dynamical core experiment.
 - Comparing with the results of the spectral model AFES, our model generated the almost same results.
- The computational performance of our model was measured on the Earth Simulator.
 - We obtained an ideal scalability and a good sustained performance (40% of peak performance).
 - Comparing with the performance of AFES (as one of spectral model), we guess that gridpoint models may be superior to spectral models in the higher resolution than 30km resolvable scale.



- It's difficult to do trial and error for tuning the microphysics scheme in the development stage.
 - For this purpose, we use a stretched icosahedral grid by the Schmidt transformation.
- We have shown the application of the stretched grid to the tropical squall line case.
 - Lin et al.(1983) scheme generates the reasonable squall line qualitatively
- After enough assesment of the scheme, we will perform the global cloud resolving runs.
 - Aqua Plant Experiment
 - Realistic topography run

